New Research Proposal to Jefferson Lab PAC 30

Probing the Proton's Quark Dynamics in Semi-Inclusive Pion Production at 12 GeV

H. Avakian[1],P.Bosted, S. Boyarinov, V.D. Burkert, L. Elouadrhiri,
R. Niyazov, Yu. Sharabian
Jefferson Lab, Newport News, VA 23606, USA

Z.-E. Meziani[1], B. Sawatzky, A. Lukhanin
Temple University 1900 N. 13th St.Philadelphia, PA 19122, 6082, USA

J. Annand, D. Ireland, R. Kaiser, K. Livingston, D. Protopopescu, G. Rosner, B. Seitz[1]
Univ. of Glasgow, Glasgow G12 8QQ, UK

K. Joo[1], M. Ungaro
University of Connecticut, Storrs, CT 06269, USA

K. Griffioen
College of William & Mary, 23187, USA

A. Biselli
Fairfield University, Fairfield CT 06824, USA

N. Kalantarians
University of Houston, Houston, TX 77004, USA

V. Kubarovsky, P.Stoler
Rensselaer Polytechnic Institute, Troy, NY 12181, USA

X. Jiang
Rutgers University, Piscataway, NJ. 34000, USA

O. Pogorelko, S. Kuleshov, I. Bedlinsky
Institute of Theoretical and Experimental Physics, Moscow, 117259, Russia

G. Fedotov, B. Ishkhanov, V.Chesnokov, E. Isupov,V. Mokeev, N. Shvedunov
119899 Vorob'evy gory, Skobeltsyn Nuclear Physics Institute at MSU,Moscow, Russia

A. Afanasev
Hampton University, Hampton, VA 23668

M. Anselmino, A. Kotzinian, A. Prokudin
Università di Torino and INFN, Sezione di Torino, Via P. Giuria 1, I-10125 Torino

F. Yuan
RBRC, Brookhaven National Laboratory, Upton, NY 11973, USA

M. Burkardt
New Mexico State University, PO Box 30001, Las Cruces, NM 88003, USA

[1]Co-spokesperson

L. Gamberg
Penn State Berks , Tulpehocken Road, Reading, PA 19610, USA
G.R. Goldstein
Tufts University, Medford, MA 02155, USA
Ph. Hägler
Technische Universität München, D-85747 Garching, Germany
A. Schäfer
Universität Regensburg, D-93040 Regensburg, Germany
G. Schierholz
NIC, DESY, D-15738 Zeuthen, Germany
J.M. Zanotti
University of Edinburgh, Edinburgh EH9 3JZ, UK

Abstract

We propose to study azimuthal asymmetries in semi-inclusive electroproduction of pions using the JLab 12 GeV polarized electron beam and the CLAS12 detector with an unpolarized hydrogen target.

The measurement of the $\cos 2\phi$ azimuthal moment of the cross section, in particular, will probe the Collins fragmentation function and will also provide information on the orbital motion of quarks by determining the leading-twist Boer-Mulders transverse-momentum-dependent (TMD) parton distribution, related to the interference between $L = 0$ and $L = 1$ light-cone wave functions.

The $\sin\phi$ and $\cos\phi$ moments will also be analyzed, further probing the transverse momentum distributions of partons and allowing the study of the higher-twist contributions. The P_T and Q^2-dependences of the $\cos 2\phi$, $\sin\phi$, and $\cos\phi$ moments will be studied to test the transition from a non perturbative description at low P_T to a perturbative description of the process at high P_T. High-statistics measurements of semi-inclusive pion production will be used to study the $(Q^2, W, x, P_\perp, z)$ phase space, where factorization of PDFs and fragmentation functions holds. Two-pion production will also be studied to help understand the diffractive ρ^0 and other two-pion contributions to semi-inclusive deep inelastic scattering.

A total of 2000 beam hours is requested. The experiment makes use of the base equipment in Hall B, including the CLAS12 and ancillary beamline instrumentation.

Technical participation of research groups

Temple University

Temple University's group has one faculty member (Z.-E. Meziani), a post-doc(B. Sawatzky), a research associate (A. Lukhanin) and several graduate students. The major source of funding for the group is DOE, however, the research associate is only paid half by DOE the other half of his salary is provided by the University. The intended contribution is 1 FTE-year for the Cherenkov counter installation and commissioning as well as the analysis of the experiment.

The Glasgow University

The Glasgow University group is actively involved in this proposal, as well as in another proposal using CLAS12, one proposal for Hall A and the GlueX proposal.

The Glasgow group plans to contribute to the design, prototyping, construction and testing of the following CLAS12 baseline equipment: silicon vertex tracker electronic readout system, data acquisition, GRID computing, photon beamline. Beyond the baseline equipment, the group is also interested in building a RICH detector for kaon identification in CLAS12.

Seven faculty members and research staff and four technicians/engineers are likely to work at least part time on this project in the next few years. Funding for the group is from the UK Engineering and Physical Sciences Research Council, EPSRC. Additional sources of funding will be sought as appropriate.

University of Connecticut

The University of Connecticut (UConn) group is actively involved in this proposal using CLAS12 baseline equipment.

Among the CLAS12 baseline equipment, our group is sharing the responsibility for the design, prototyping, construction and testing of the high threshold cerenkov counter (HTCC). One faculty member (Kyungseon Joo), one post-doc (Maurizio Ungaro), four graduate students (Bo Zhao, Nikolay Markov, Taisia Mineeva and Igor Konyukov) are already or will be working on this project.

The University of Connecticut Research Foundation (UCRF) already funded $32,000 for the equipment purchase for the HTCC prototyping project. UConn is also providing a clean room facility for this project and providing funding for a half postdoctoral support and a half graduate student support for the next two years for our group's JLab research activities. The group is currently funded by the U.S Department of Energy (DOE). Additional sources of funding will be sought as appropriate.

Beyond the baseline equipment, the group is also deeply involved in software planning and development for CLAS12. The group was recently awarded a DOE

SBIR/STTR Phase I grant with a software company, CyberConnect EZ to develop a software framework to archive a large scale nuclear physics experiment data base.

Contents

1 Introduction

Inclusive deep inelastic scattering processes probe the longitudinal momentum distribution of the nucleon. In the last few years it became clear that hard exclusive and semi-inclusive processes can provide information on transverse momentum of quarks and transverse distance of a quark from the center of mass of the nucleon, enabling the so-called " nucleon tomography", or scanning the nucleon in transverse slices.

Azimuthal distributions of final state particles in semi-inclusive deep inelastic scattering play a crucial role in the study of transverse momentum distributions of quarks in the nucleon and provide access to the orbital motion of quarks.

In perturbative QCD, which applies when the transverse momentum $P_\perp$ of the detected hadron is large compared to Λ_{QCD}, asymmetries vanish at leading twist level. The observed spin-dependent and spin-independent azimuthal asymmetries occur at $P_\perp$ below 1-2 GeV, which is not much larger than Λ_{QCD} or the typical parton transverse momenta of the order of 0.5 GeV. Thus the asymmetries could arise from non-collinear parton configurations or from multi-parton correlations ("higher twist" effects, which are suppressed at large $P_\perp$). Presently, the intrinsic transverse momentum of partons in the nucleon plays the crucial role in most explanations of non-zero azimuthal asymmetries in hadronic reactions [1, 2, 3, 4, 5, 7].

In recent years significant progress has been made in understanding the role of partonic initial and final state interactions [8, 9, 10]. The interaction between the active parton in the hadron and the spectators leads to gauge-invariant transverse momentum dependent (TMD) parton distributions [8, 9, 10, 11, 12]. The universality of the TMD correlation functions has been proved resulting in a sign change for two T-odd TMD distributions between Drell-Yan and DIS [9, 14]

Furthermore, QCD factorization for semi-inclusive deep inelastic scattering at low transverse momentum in the current-fragmentation region has been established in Refs. [13, 14]. A detailed verification of factorization and calculations of the relevant factors in the factorization formulas have also been carried out in Ref. [13]. This new framework provides a rigorous basis to study the TMD parton distributions from SIDIS data using different spin-dependent and independent observables. TMD distributions (see Table 1) describe transitions of a nucleon with one polarization in the initial state to a quark with another polarization in the final state.

The diagonal elements of the table are the momentum, longitudinal and transverse spin, distributions of partons, and represent well-known PDFs related to the square of the leading-twist light-cone wave functions. Off diagonal elements require non-zero orbital angular momentum and are related to the wave function overlap of L=0 and L=1 Fock states of the nucleon [15]. Two combinations of this interference appear. Chiral even distributions $f_{1T}^\perp$ and g_{1T} are the imaginary and real parts of one interference term and chiral odd $h_1^\perp$ and h_{1L} are imaginary and real parts of the second interference term respectively. The TMDs $f_{1T}^\perp$ and $h_1^\perp$, related to the

Table 1: Leading twist transverse momentum dependent distribution functions. The U,L,T stand for transitions of unpolarized, longitudinally polarized and transversely polarized nucleons (rows) to corresponding quarks (columns).

N/q	U	L	T	
U	$\mathbf{f_1}$		$h_1^\perp$	
L		$\mathbf{g_1}$	$h_{1L}^\perp$	
T	$f_{1T}^\perp$	g_{1T}	$\mathbf{h_1}$	$h_{1T}^\perp$

imaginary part of the interference of wave functions for different orbital momentum states and known as the Sivers and Boer-Mulders functions [16, 17, 18, 9, 10, 11], describe unpolarized quarks in the transversely polarized nucleon and transversely polarized quarks in the unpolarized nucleon respectively. They vanish *at tree-level* in a T-reversal invariant model (T-odd) and can only be nonzero when initial or final state interactions cause an interference between different helicity states. During the last few years, first results of the Sivers function have become available [5, 6]. This function parameterizes the correlation between the transverse momentum of quarks ejected from a transversely polarized target and the transverse spin of the nucleon. What makes the Sivers function so interesting is that it requires both orbital angular momentum as well as non-trivial phases from the final state interaction that survives in the Bjorken limit. Experimental results of the Sivers functions for up and down quarks are consistent with a heuristic model of up and down quarks orbiting the nucleon in opposite directions.

The Boer-Mulders (BM) function describes the correlation between the transverse spin and momentum of a quark ejected from an unpolarized target in SIDIS. It is thus similar to the Sivers function except that the nucleon spin is swapped for the spin of the active quark. Like the Sivers function, it arises from an interference between final state interaction phases from states that differ by one unit of orbital angular momentum. The most simple mechanism that can lead to a BM function is a correlation between the spin of the quarks and their orbital angular momentum. In combination with a final state interaction that is on average attractive, already a measurement of the sign of the BM function would thus reveal the correlation between orbital angular momentum and spin of the quarks. **This information, together with independent measurements related to the spin and orbital angular momentum of the quarks will help construct a more complete picture about the spin structure of the nucleon**.

The impact parameter space displacement of transversely polarized quark distributions in an unpolarized target is described by a chirally odd GPD [19], and has recently been calculated for the first time in lattice QCD [20]. The resulting transverse flavor dipole moment for transversely polarized quarks in an unpolarized nucleon

was found to be at least 1.5 times as large as the corresponding dipole moment for unpolarized quarks in a transversely polarized target.

This result suggests Boer-Mulders functions that are significantly larger than Sivers functions (see Fig. 1). Moreover, consistent with large N_C predictions, the displacement of transversely polarized u and d quarks was found to be in the same direction, indicating the same sign for the BM functions for u and d quarks, and suggesting a further enhancement of the SIDIS asymmetry from the d quark contribution.

Similar to the Boer-Mulders distribution function, other quantities arise in the hadronization process. One particular case is the Collins T-odd fragmentation function $H_1^\perp$ [36] which gives the probability of a transversely polarized quark fragmenting into unpolarized hadrons.

1.1 Azimuthal Moments in SIDIS

The azimuthal angle ϕ dependence of hadrons produced in lepton scattering off a polarized nucleon probes the quark transverse spin distribution [36]. Within the one photon exchange approximation, the double inclusive cross section for unpolarized SIDIS processes, $\ell p \to \ell h X$, can have a dependence on the azimuthal angle ϕ_h of the final hadron already at leading order. The cross section (see for ex.[13]) has contributions from two structure functions:

$$\frac{d\sigma}{dx_B dQ^2 dz_h d^2\vec{P}_{h\perp}} = \frac{4\pi\alpha_{\rm em}^2}{Q^4}\left[(1-y+y^2/2)F_{UU}^{(1)} + (1-y)\left(-\cos(2\phi_h)F_{UU}^{(2)}\right)\right] , \quad (1)$$

where $F_{UU}^{(1)}$ depends on unpolarized quark distribution and fragmentation functions, and $F_{UU}^{(2)}$ on the Boer-Mulders function: $h_1^\perp$ and the Collins fragmentation function $H_1^\perp$. According to the transverse momentum dependent factorization the structure functions factorize into TMD parton distributions and fragmentation functions, and into soft and hard parts [13]. The $F_{UU}^{(2)}$ thus can be written as

$$F_{UU}^{(2)} = \int d^2\vec{k}_\perp d^2\vec{p}_\perp d^2\vec{\lambda}_\perp \delta^{(2)}(z\vec{k}_\perp + \vec{p}_\perp + \vec{\lambda}_\perp - \vec{P}_{h\perp}) \frac{2\vec{k}_\perp\cdot\hat{\vec{P}}_{h\perp}\vec{p}_\perp\cdot\hat{\vec{P}}_{h\perp} - \vec{k}_\perp\cdot\vec{p}_\perp}{MM_h}$$
$$\times h_1^\perp(x_B,k_\perp)\, H_1^\perp(z_h,p_\perp)\, S(\vec{\lambda}_\perp) H_{UU}^{(2)}\left(Q^2\right) . \quad (2)$$

The hard factor, H_{UU}, is calculable in pQCD, and the soft factor $S(\vec{\lambda}_\perp)$ comes from soft gluon radiation and is defined by a matrix element of Wilson lines in the QCD vacuum [13].

The kinematics of the interaction is illustrated in Fig. 2 The incoming (l) and outgoing (l') lepton lines, along with the virtual photon (q) direction define the lepton

scattering plane. The angle ϕ_h (ϕ) is the azimuthal angle of the pion around the virtual photon direction with $\phi_h = 0$ in the positive x axis direction.

The relevant kinematic variables are defined as:

$$-Q^2 = (l - l')^2, \quad \nu = \frac{p \cdot q}{M} = E - E', \quad W^2 = 2M\nu + M^2 - Q^2,$$

$$x_B = \frac{Q^2}{2pq}, \quad y = \frac{\nu}{E}, \quad z = \frac{E_\pi}{\nu}, \quad x_F = \frac{2P_L}{W},$$

where (l) and (l') are 4-momenta, and E, E', the laboratory energies of incoming and outgoing leptons, respectively. E_π is the pion laboratory energy and M the proton mass. The transverse (P_T) and longitudinal (P_L) momentum of the pion are defined with respect to the virtual photon direction (CMS), $k_\perp$ and $p_\perp$ are quark transverse momenta before and after scattering, and P_1 and P_h are the four momenta of the initial nucleon and the observed final-state hadron, respectively. Positive and negative values of the x_F define the current fragmentation region and the target fragmentation region respectively.

Within the leading order (zero-th order in α_s) parton model with twist-two distribution and fragmentation functions (FFs), the simplest azimuthal asymmetry, a $\cos\phi_h$ dependence, arises in unpolarized SIDIS (the so-called Cahn effect [21]). It is related to the quark intrinsic transverse motion, $\boldsymbol{k}_\perp$, and gives a kinematical correction to the usual cross-section, computed in collinear configuration, proportional to $k_\perp/Q$. The study of the cross-section dependence on $\cos\varphi_h$ and on P_{hT} allows to extract the parameters describing the unpolarized TMD DFs, $f_1^q(x, \boldsymbol{k}_\perp^2)$, and FFs, $D_q^h(x, \boldsymbol{p}_\perp^2)$ (for a recent analysis see [22], where the Sivers asymmetry was also analyzed).

Within the same approach, kinematical corrections proportional to $(k_\perp/Q)^2$ lead to additional contributions in the $\cos 2\phi_h$ moment. Both Cahn and Boer-Mulders effects are contributing with the same sign, enhancing the $\cos 2\phi_h$ asymmetry. In order to extract the contribution of the Boer-Mulders + Collins part one needs a reliable calculation of the kinematical corrections. Perturbative QCD contributions (at order α_s and possibly α_s^2) to the kinematical $\cos\phi_h$ and $\cos 2\phi_h$ asymmetries also have to be evaluated. Such a study shows that the parton model with TMD DFs and FFs dominates at P_{hT} values below 1 (GeV/c) [22].

Proposed studies include the dependence of the unpolarized SIDIS cross-section on 1) P_{hT}, 2) $\cos\phi_h$, 3) $\cos 2\phi_h$. A careful analysis of the data from points 1) and 2), in particular at small P_{hT} values, will lead to a consistency check of the overall scheme and to a better extraction of the parameters describing the $\boldsymbol{k}_\perp$ and $\boldsymbol{p}_\perp$ dependence of the DFs and FFs, respectively. Having achieved that, one has a full control on the kinematical azimuthal asymmetries and can therefore exploit the data from point 3) to extract the parameters of the Boer-Mulders DFs and Collins FFs. This should be done by using, in addition, the combined data from HERMES, COMPASS and BELLE.

It is important to stress that a good knowledge of the unpolarized and unintegrated DFs and FFs is needed in order to extract further information on other polarized DFs

like $g_{1T}^q(x, \boldsymbol{k}_\perp^2)$ [23] and $g_{1L}^q(x, \boldsymbol{k}_\perp^2)$ [24], and to check general positivity bounds [25] and Lorentz invariance relations. Besides, the study of other azimuthal asymmetries in polarized SIDIS, like $A_{LL}^{\cos\phi_h}$, which gives access to $g_{1L}^q(x, \boldsymbol{k}_\perp^2)$, demands the precise knowledge of the unpolarized $\cos\phi_h$ asymmetry.

We propose a measurement of azimuthal moments of the single pion cross section in SIDIS using the CLAS12 [26] in Hall B at Jefferson Lab, a 6.6-11.0 GeV longitudinally polarized electron beam and an unpolarized hydrogen target. The focus of our proposal is to study the $\cos 2\phi$ asymmetry, related to the correlation of intrinsic transverse momentum of quarks and their transverse spin. Competing mechanisms are also related to the transverse motion of quarks and are also relevant in the CLAS12 kinematic regime ($\langle Q^2 \rangle \sim 2$ GeV^2). We propose to run with high luminosity, $\sim 10^{35}$ cm^{-2}s^{-1}, yielding an integrated luminosity of ~ 500 fb^{-1}.

2 The $\cos 2\phi$ asymmetry in unpolarized SIDIS

Four possible mechanisms generating the $cos2\phi$ moment have been identified : 1) non-collinear kinematics at order k_T^2/Q^2 [21]; 2) perturbative gluon radiation [27, 28, 29, 30]; 3) higher-twist semi-exclusive pion production, when the final meson is produced at short distances via hard-gluon exchange [32, 33, 34]; 4) the leading-twist Boer-Mulders function [35] coupling to Collins function [36]:

$$\sigma_{UU}^{\cos 2\phi} \quad \propto \quad 2(1-y)\cos 2\phi \sum_{q,\bar{q}} e_q^2 x h_1^{\perp q}(x) H_1^{\perp q}(z), \tag{3}$$

The unpolarized fragmentation function, D_1, and polarized fragmentation function,$H_1^\perp$, describing the fragmentation of transversely polarized quarks into unpolarized hadrons, depend in general on the transverse momentum of the fragmenting quark relative to the outgoing hadron.

The physics of $\sigma_{UU}^{\cos 2\phi}$, which involves the Collins fragmentation function $H_1^\perp$ and Boer-Mulders distribution function $h_1^\perp$, was first discussed by Boer and Mulders in 1998 [35]. In recent years, the $\cos 2\phi$ asymmetry in leptoproduction was phenomenologically studied using different approximations for the Boer-Mulders function [38, 39, 40].

Independent information on the Boer-Mulders function $h_1^\perp(x, \mathbf{k}_T^2)$ can be obtained from the study of the $\cos 2\phi$ azimuthal asymmetry in unpolarized Drell-Yan processes, which has been measured in πN collisions [41, 42]. In [43, 44] this asymmetry was estimated by computing the $h_1^\perp$ distribution of the pion and of the nucleon in a quark spectator model [45, 46]. The $\cos 2\phi$ azimuthal asymmetry in SIDIS was computed assuming that the π^+ production is dominated by u quarks and using the same distributions $h_1^\perp(x, \mathbf{k}_T^2)$ and $f_1(x, \mathbf{k}_T^2)$ used in [44].

The calculation of the $\cos 2\phi$ asymmetry appeared to be in rather good agreement for low values of the P_T (up to 0.5 GeV) with SIDIS data coming from the ZEUS

experiment [47] at large Q^2 values ($0.01 < x < 0.1$, $0.2 < y < 0.8$, $0.2 < z < 1$, $Q^2 > 180$ GeV^2) where the higher twist contribution are not expected to be relevant (see Fig. 3).

The Boer-Mulders contribution, being leading twist, is expected to survive at higher Q^2 and that can be tested at large Q^2 accessible with CLAS12.

At large transverse momentum, i.e., $P_{h\perp} \gg \Lambda_{\rm QCD}$, the transverse momentum dependence of the various factors in the factorization formula (Eq.2) may be calculated from perturbative QCD. Following the similar arguments in Ji-Qiu-Vogelsang-Yuan [48], the Boer-Mulders function will have the following power behavior at large transverse momentum,

$$h_1^\perp(x, k_\perp)|_{k_\perp \gg \Lambda_{\rm QCD}} \propto \frac{M_P}{(k_\perp^2)^2} \ . \tag{4}$$

Similarly, the Collins function $H_1^\perp(z, p_\perp)$ has the same power behavior at large $p_\perp$,

$$H_1^\perp(z, p_\perp)|_{p_\perp \gg \Lambda_{\rm QCD}} \propto \frac{M_h}{(p_\perp^2)^2} \ . \tag{5}$$

Substituting the above results into the factorization formula gives

$$F_{UU}^{(2)}(P_{h\perp}, Q^2) \propto \frac{1}{(P_{h\perp}^2)^2} \ . \tag{6}$$

On the other hand, the unpolarized cross section contribution $F_{UU}^{(1)}$ is well known, and goes like

$$F_{UU}^{(1)}(P_{h\perp}, Q^2) \propto \frac{1}{P_{h\perp}^2} \ . \tag{7}$$

From the above analysis, the $\cos 2\phi$ azimuthal asymmetry has the following behavior at $\Lambda_{\rm QCD} \ll P_{h\perp} \ll Q$,

$$\langle \cos 2\phi \rangle|_{P_{h\perp} \gg \Lambda_{\rm QCD}} \propto \frac{1}{P_{h\perp}^2} \ . \tag{8}$$

When the transverse momentum is compatible with the large scale Q, the above results will be modified, because the gluon radiation from pQCD diagram will dominate, and contribute to the azimuthal asymmetry not being suppressed by any hard scale. At Q^2 values accessible at JLab ($1.0 < Q^2 < 10$GeV^2), however, the reduction of the Boer–Mulders asymmetry due to Sudakov form factors arising from soft gluon contributions [49] is not expected to be significant.

Measurement of the P_T dependence of the BM-asymmetry will allow for checking the predictions of a unified description of SSA by Ji and collaborators [13, 48] and study the transition from a non-perturbative to the perturbative description.

The $\cos 2\phi$ asymmetry for semi-inclusive deep inelastic scattering in the kinematic regions of CLAS12 is predicted to be significant (of order of few percent in average) and tends to be larger in the small-x and large-z region. The preliminary data from

CLAS (see Fig. 7) at 6 GeV indeed indicate large azimuthal moments both for $\cos\phi$ and $\cos 2\phi$.

The combined analysis of the future CLAS12 data on $\langle\cos 2\phi\rangle$ and of the previous ZEUS measurements in the high-Q^2 domain (where higher twist effects are negligible) will provide information on the Boer-Mulders function, shedding light on the correlations between transverse spin and transverse momenta of quarks.

2.1 Semi-Exclusive Meson Production

In the processes of semi-exclusive electroproduction, the final meson is produced at short distances via hard-gluon exchange [31, 32, 33, 34], with a characteristic rapidity gap between the current fragmentation region and target fragmentation region. First discussed by Berger[31], this mechanism is expected to dominate the cross section in the kinematic regime where the ejected meson picks up most of the virtual photon momentum (large z) [33]. Phenomenological fragmentation functions are not required to describe this important class of deep-inelastic processes, since the mechanism of meson production from a quark is described exactly by pQCD. It is essential that in the theory of semi-exclusive reactions, formation of the final hadronic state is described in terms of quark distribution amplitudes, therefore providing a connection between inclusive and exclusive reactions (see Fig. 4). It was also noted that with CEBAF upgraded to 12 GeV, the semi-exclusive channel allows one to reach high virtuality of the exchanged gluon, corresponding to about $Q^2 \sim$30 GeV^2 for the exclusive case of the pion form factor [50].

It was shown in Ref.[32] that higher twist effects may be isolated in semi-exclusive pion production for moderate values of Q^2. Significant $\cos\phi$ and $\cos 2\phi$ moments (see Fig.5) were predicted in the exclusive limit ($z \to 1$).

The study of HT contribution apart from being an important background to BM-contribution, provides an important first step in solving the problem of meson formation in hard processes.

An important physics implication of the connection between inclusive and exclusive reactions is that the corresponding subprocess, $\gamma^* q \to \pi q$, is an essential component of the formalism of Deeply Virtual Meson production. Semi–inclusive measurements may therefore produce model–independent information necessary to extract (polarized) Generalized Parton Distributions from deeply–virtual exclusive electroproduction of mesons.

The CLAS12 detector can provide complete kinematic coverage of semi-exclusive electroproduction reactions in the deep-inelastic region.

2.2 Beam Spin Asymmetry

The Boer-Mulders distribution function coupled with a higher twist fragmentation function [51, 52] contributes also to the beam spin dependent $\sin\phi$ moment. Assum-

ing factorization holds, the beam single-spin asymmetry measurements can provide independent information on the transverse momentum distributions of quarks. The contribution to beam SSA arising at distribution level and independent on quark fragmentation process was first discussed by Afanasev and Carlson [53]. The distribution function responsible for that contribution was later identified by Bacchetta et al [54]:

The beam SSA first extracted at CLAS [7] at 4.3 GeV is consistent with measurements at HERMES [55]. This data analyzed in terms of the Collins effect [56] provided first glimpse of the essentially unknown twist-3 distribution function $e(x)$.

In jet SIDIS with massless quarks, when the fragmenting quark momentum is measured directly, all contributions, arising in the fragmentation process, vanish and the beam SSA is directly proportional to the T-odd distribution function $g^{\perp}$. Assuming the favored and unfavored polarized FFs are approximately equal and opposite in sign, as indicated by the HERMES measurement of large transverse asymmetries for π^- [5], the contribution proportional to the Collins function will be suppressed for π^0 and the sum of π^+ and π^-. That may allow model independent extraction of $g^{\perp}$ from beam SSA measurements with proton and deuteron targets.

Beam SSAs do not require polarized targets and are free of dilution. They could be measured at the highest accessible luminosities. This makes them an important tool for factorization studies using measurements of different final state hadrons.

2.3 Target Fragmentation

The wide kinematic coverage of CLAS12 combined with high beam polarization and high luminosity, allows precision measurements of semi-inclusive processes in the target fragmentation region (TFR). The TFR corresponds to the backward hemisphere in the CM frame requiring negative values for Feynman variable, x_F, defined as a longitudinal fraction of the hadron momentum in CM frame. The momentum conservation requires that the transverse momentum of the current quark is balanced by that of the target remnant, which in turn means that the azimuthal angle of the target remnant $\varphi_{qq} = \varphi + \pi$. This leads to observable azimuthal asymmetries in the target fragmentation region [57] (see Fig. 6).

3 Experimental situation

The goal of the proposed experiment is to measure the kinematic dependence of azimuthal moments in pion production in SIDIS and in particular the $\cos 2\phi$ moment of the target spin-independent cross section. This will be the first statistically significant measurement of kinematic dependences for the Boer-Mulders TMD distribution in SIDIS. The $\cos\phi$ and $\sin\phi$ moments will also be studied to establish their twist-3 nature from their Q^2 and P_T dependences.

3.1 Existing Data on Unpolarized Moments

First studies of azimuthal moments in SIDIS were reported by the European Muon Collaboration at CERN. EMC measured $\langle \cos 2\phi \rangle$ for $Q^2 > 4$ GeV^2 [58]. Azimuthal moments in SIDIS of 490 GeV muons were studied at Fermilab experiment E665 [59]. At HERA both HERMES [60] and ZEUS [47] performed studies of unpolarized azimuthal moments in a wide range of kinematics. The existing data, however, are affected by large uncertainties and do not allow drawing definite conclusions about the magnitude and the shape of the asymmetry.

Significant azimuthal moments (both $\cos\phi$ and $\cos 2\phi$) were measured with CLAS at 6 GeV (see Fig. 7), however, the limited range in Q^2 and P_T makes the interpretation of the data model dependent.

3.2 Overview of the experiment

We propose to scatter longitudinally polarized high energy electrons off unpolarized protons. Although the focus of the proposed experiment is the study of azimuthal moments of π^+ and π^-, π^0's will be measured as well, and used as a cross check. The acceptance for scattered electrons is shown in Fig. 8. At 11 GeV higher missing mass values and higher P_T of hadrons are accessible, significantly extending the kinematic range for SIDIS studies.

3.2.1 Trigger, data acquisition, PID and reconstruction

We are planning to use the standard CLAS12 production trigger, data acquisition, and online monitoring system of CLAS12. The standard electron trigger consists of a time coincidence between the High Threshold Cherenkov Counter (HTCC) and an energy deposition in the forward electromagnetic calorimeter (EC) in a given sector. The signal amplitude and time information will be read out using standard ADC and TDC boards currently in use in CLAS. The expected data acquisition rate is about 10 kHz, which can be handled by the DAQ with a reasonably small computer dead time. Additional pre-scaled triggers will be used to calibrate the Cherenkov and EC efficiencies for electrons.

Event identification in CLAS12 will be accomplished using charged particle tracking in the toroidal magnetic field, a signal (or absence of signal in the HTCC and LTCC), time-of-flight, and momentum information. Electrons are separated from heavier particles using threshold gas Cherenkov detectors, the preshower and the electromagnetic calorimeter.

Neutral pions will be identified using their decay to two photons. Photons are separated from neutrons by requiring their velocity $\beta > 0.9$, as measured with the calorimeter time. Their energy is determined from the normalized calorimeter (IC or EC) energy. A neutral pion is identified if the invariant mass squared of the two photons passes the cut $0 < M^2_{\gamma\gamma} < 0.03$ GeV^2.

3.3 MC studies of azimuthal moments

Realistic MC simulations are crucial for separation of different contributions to $\cos\phi$ and $\cos 2\phi$ azimuthal moments arising from higher twists, radiative corrections [61] and in particular from the detector acceptance. The CLAS12 FAST-MC program was used to simulate the physics events and study the extraction of azimuthal moments and acceptance corrections.

The SIDIS cross section assuming Gaussian $k_\perp$ and $p_\perp$ dependence, both for parton densities and fragmentation functions the cross section including only kinematic HT to the lowest order in P_T/Q is given by:

$$\frac{d^5\sigma^{\ell p\to\ell h X}}{dx_B\, dQ^2\, dz_h\, d^2\mathbf{P}_T} \simeq \sum_q \frac{2\pi\alpha^2 e_q^2}{Q^4}\, f_q(x_B)\, D_q^h(z_h)\Big[1+(1-y)^2 + \frac{4\mu_0^2(1-y)}{\mu_H^2 Q^2}(\mu_D^2 + \frac{z^2\mu_0^2 P_T^2}{\mu_H^2}) - 4\,\frac{(2-y)\sqrt{1-y}\,\mu_0^2\, z_h\,|\vec{P_T}|}{\mu_H^2\, Q}\,\cos\phi_h + \frac{4\mu_0^4 z^2(1-y)P_T^2}{\mu_H^4 Q^2}\cos 2\phi_h\Big]\frac{1}{\pi\mu_H^2}\, e^{-P_T^2/\mu_H^2}\ , \quad (9)$$

where $\mu_H^2 = \mu_D^2 + z_h^2\mu_0^2$ and μ_0^2 and μ_D^2 are average transverse momentum widths in distribution and fragmentation, respectively. The terms proportional to $\cos\phi_h$ and $\cos 2\phi_h$ describe the Cahn effect [21]. The Cahn effect (also Sivers effect) were included in LEPTO MC by Kotzinian [57]. The acceptance effects were studied using two alternative approaches, with different sensitivity to detector acceptance.

3.3.1 Extraction of $\cos 2\phi$, $\cos\phi$ and $\sin\phi$ moments

An important part of the experiment will be to extract the $\cos 2\phi$ ($A^{\cos 2\phi}$), $\cos\phi$ ($A^{\cos\phi}$) and $\sin\phi$ ($A^{\sin\phi}$) moments as functions of Q^2, x_B P_T and z_h. To estimate the accuracy we will be able to achieve in the measurement of response functions, events were then generated with $A^{\cos\phi} = -0.2$, $A^{\cos 2\phi} = 0.1$, and $A^{\sin\phi} = 0.1$. These were then fed through *FastMC* to obtain the simulated detector "data". The "data" were then acceptance corrected to obtain the differential cross sections. These cross sections were then fit by a function $A(1 + Bcos2\phi + Ccos\phi)$, where A, B, and C are related to the individual moments. The fits to the cross sections for $Q^2 = 2.0$ GeV^2 are shown in Figure 9. Beam spin asymmetries are also simulated by extracting $(N^+ - N^-)/(N^+ + N^-)$ for each bin where $N^\pm$ are the number of events from $\pm$ electron helicity. These asymmetries were then fit by a function $Asin\phi/(1+Bcos2\phi+Ccos\phi)$, where A is related to the $A^{\sin\phi}$ moment. The fits to the asymmetries for Q^2= 2 GeV^2 are also shown in Figure 10. It is clearly demonstrated that the $A^{\cos\phi}$, $A^{\cos 2\phi}$, and $A^{\sin\phi}$ moments can be extracted over a very large kinematic range.

3.3.2 Extraction of $\cos 2\phi$, $\cos\phi$ using acceptance moments

Figures 11,13 show all relevant moments extracted for the π^+ and π^- acceptance (no initial ϕ-modulation in the generated sample) and the cross section. Detailed knowledge of azimuthal moments of the acceptance allow extraction of the cross section moments from measured azimuthal moments (see Appendix). Using just the first two moments of the acceptance already provides a reasonable extraction of Cahn moments (see Fig.12).

3.4 Projected results and impact on physics

The precision measurement of the Boer-Mulders asymmetry requires subtraction of all above discussed contributions to the $\cos 2\phi$ moment. All contributions, including the Cahn and Berger terms as well as the perturbative and radiative contributions to first order are expected to be "flavor blind", i.e. are the same for negative and positive pions. The check performed with the $\cos\phi$ moment can serve as a test for that. Contributions to $\cos\phi$ moment are also related to contributions to $\cos 2\phi$ and their extraction will provide an additional check for the background contributions to $\cos 2\phi$ being under control. Extraction of $\cos\phi$ and $\cos 2\phi$ moments for all 3 pions will provide additional information on widths of k_T distributions and their flavor dependence. The difference of the $\cos 2\phi$ moments for π^+ and π^- will provide direct access to the Boer-Mulders distribution function, assuming the Collins function is known. Measurement of the $\sin 2\phi$ moment of the cross section, or the Kotzinian-Mulders asymmetry with longitudinally polarized target[62] and the Collins effect with transversely polarized target [36] are also planned with CLAS12 and will provide independent information on the Collins function, appearing there convoluted with Mulders function [63] and transversity [64], respectively. Another important independent source of Collins function is the measurement performed at BELLE [65].

Projections for some of the most important observables in some bins are shown on Figs. 14-15. The resulting Q^2 dependences of the $\cos 2\phi$ moment (leading twist) for all pions are shown on Fig. 14. High-precision measurement will define whether the asymmetry stays constant at large Q^2, as predicted by pQCD [13]. The new data will allow more precise tests of the factorization ansatz and the investigation of the Q^2 dependence of both $\cos 2\phi$ and $\cos\phi$ asymmetries. This will enable us to study the leading-twist and higher-twist nature of both observables.

The higher statistics of CLAS12 using polarized beams (CLAS12) will allow the extraction of the transverse momentum, P_T and Q^2-dependence of the beam SSAs at fixed x_B and z (Fig.16). This will enable us to further examine the factorization hypothesis and to study the higher-twist nature of the process and probe the transition from non-perturbative (low P_T) to perturbative (high P_T) regimes of QCD. In case the contribution from the T-odd distribution function ($g^\perp$), dominates the beam-spin dependent part of the cross section the beam SSA in the perturbative limit will behave as $1/P_T$, decreasing slower than the $\cos 2\phi$ contribution with BM PDF.

Table 2: Expected systematic uncertainties for azimuthal moments

Source	$\Delta A^{cos\phi}$	$\Delta A^{cos2\phi}$	$\Delta A^{sin\phi}$
Beam polarization			2%
ϕ acceptance	3%	1%	1%
other moments	1%	2%	1%
Radiative corrections	2%	1%	1%
Total	$< 4\%$	$< 3\%$	$< 3\%$

3.4.1 Systematic errors for azimuthal moments

Compared to cross section measurements azimuthal moments are expected to be less sensitive to different sources of uncertainties due to experimental factors (acceptance, efficiencies, normalization) and physics background (radiative effects, higher twist contributions). In the cross section measurements (P_T, and ϕ-dependences) the overall systematic error is estimated to be $\sim 6-7\%$ including $\sim$4.0% due to acceptance and $\sim$3.0% due to radiative corrections. The systematic uncertainties for different moments are listed in the Table 2.

4 Summary and beam time request

In this proposal we outline a study of transverse momentum distributions of quarks and in particular the Boer-Mulders TMD parton distribution function using pion electroproduction in SIDIS for $1 < Q^2 < 11$ GeV^2, an 11 GeV electron beam, and the CLAS12 detector.

For this proposal, we assumed beam time of 2000 hours with polarized electrons at 11 GeV to access the large x, Q^2, and P_T region where the effects related to transverse momentum and spin of quarks are large. With the increased beam energy and luminosity we expect an increase of the statistics by a factor of $\sim$ 100 compared to existing HERMES and CLAS data.

In addition, the large kinematic and geometric acceptance of CLAS12 will let us study hadronic distributions in the target fragmentation region and in particular Λ production, and also accumulate a significant sample of two-pion final states. Interesting in their own right [66, 67, 68], they are also important in studies of the background to SIDIS pions from exclusive two pions and ρ in particular.

The measurements we intend to carry out are important for the future development of the formalism of TMD parton distributions, an important component of the program covered by an energy upgraded JLab. This study involves a simultaneous scan of various variables (x_B, Q^2, z, $P_\perp$ and ϕ) and for that a large acceptance detector such as CLAS12 is most suitable. Analysis of already existing electroproduction

data from the CLAS E16 experiment and studies based on simulations have shown that the proposed measurements are feasible.

The major improvement of projected error bars for pions for the dedicated measurement results from the increased acceptance for SIDIS pions (large M_X, Q^2, P_T) and higher luminosity. This will allow us to map out the x_B and z and $P_\perp$ dependence of azimuthal moments of pions in smaller bins. The proposed measurement with CLAS12 will produce precision data on the azimuthal asymmetries in SIDIS, and will provide the first significant measurement of a twist 2 TMD parton distribution which will unlikely be superseded by any ongoing or planned experiments.

Beam Request

This experiment can be carried out with 2000 hours. It does not require a polarized target and can run during the first year of operation.

The measurements involve the standard CLAS12 configuration also proposed for DVCS studies. Therefore these experiments can run simultaneously. Precise data for SIDIS asymmetries from CLAS12 will provide new and deeper insight into the nucleon structure and in particular distributions of transverse momentum and spin of quarks.

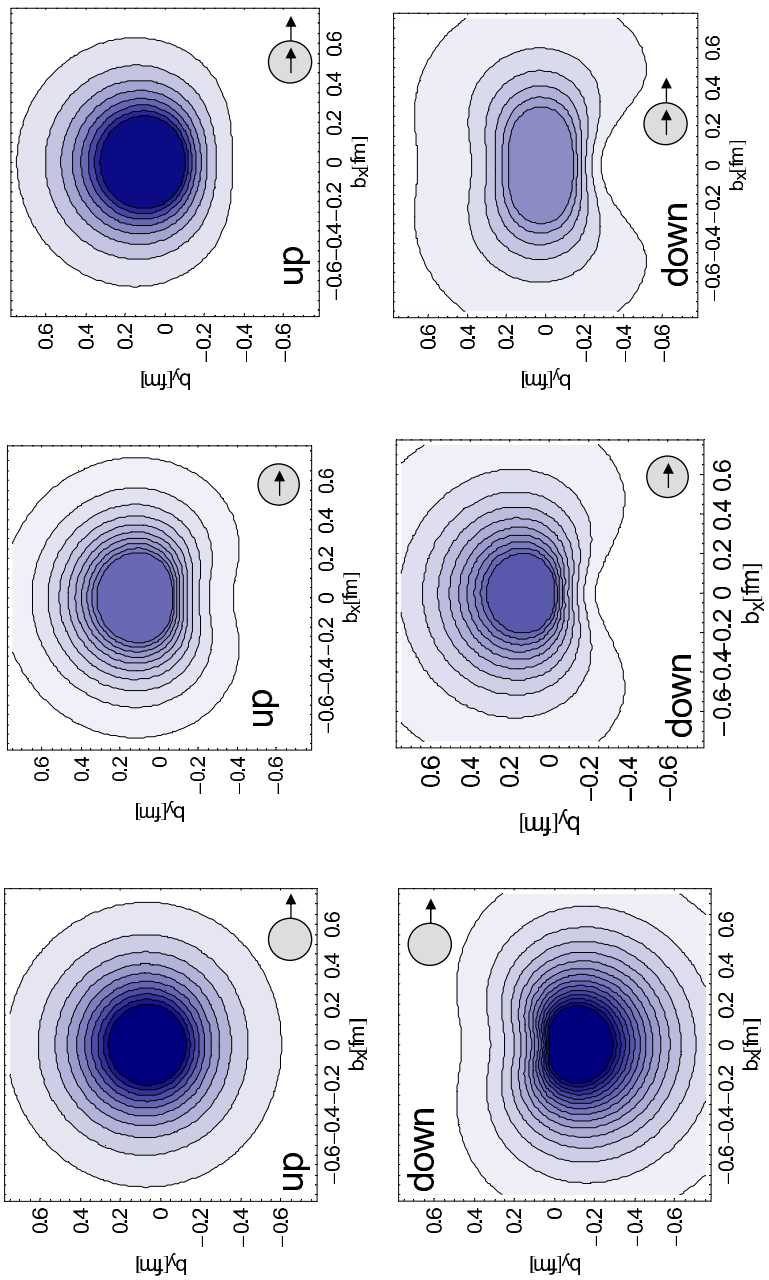

Figure 1: The lowest moment of transverse spin densities of quarks in the nucleon (Preliminary results by the QCDSF/UKQCD collaborationfrom [20]). The inner arrow represents the quark and the outer arrow the nucleon spin. The left panel shows the density of unpolarized quarks in the transversely polarized nucleon (Sivers PDF). The central plot shows the transverse deformation orthogonal to the transverse spin of quarks in the unpolarized nucleon (Boer-Mulders PDF) The right panel shows the distortions due to both transverse quark and nucleon spin

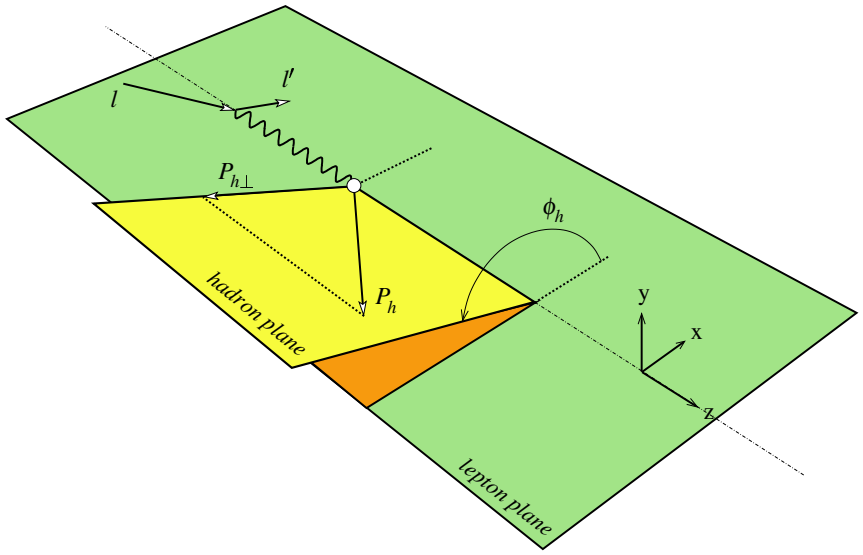

Figure 2: SIDIS kinematics.

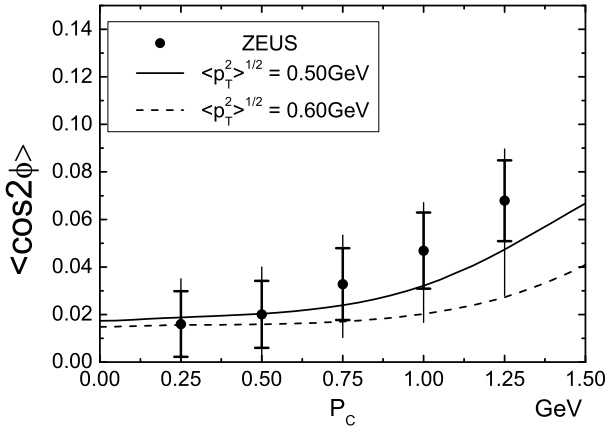

Figure 3: Comparison of calculations with ZEUS data [40]

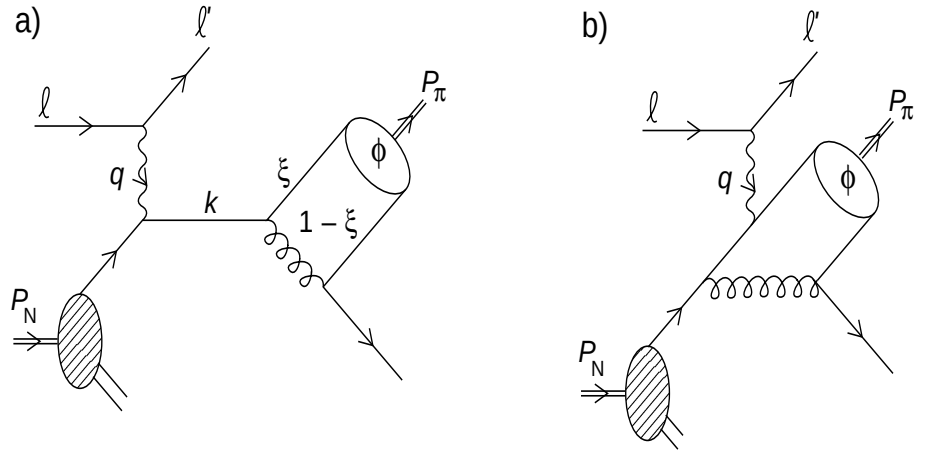

Figure 4: Leading contributions to the amplitude of the reaction $u+e^- \to e^-+\pi^++d$.

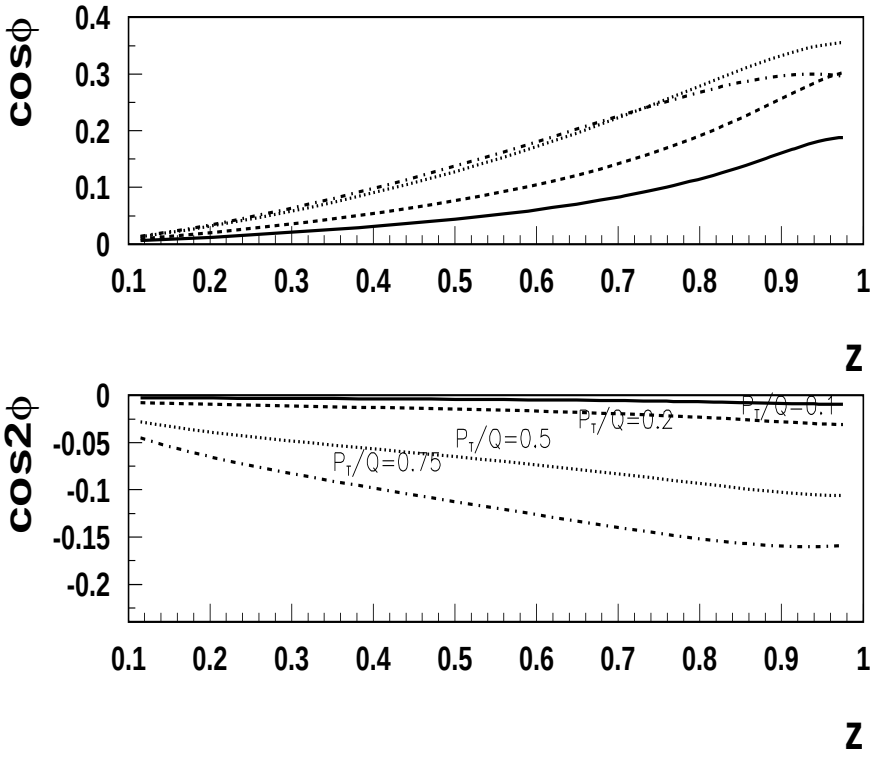

Figure 5: Azimuthal moments in unpolarized cross section as a function of z for different values of transverse momentum of the final π^+.

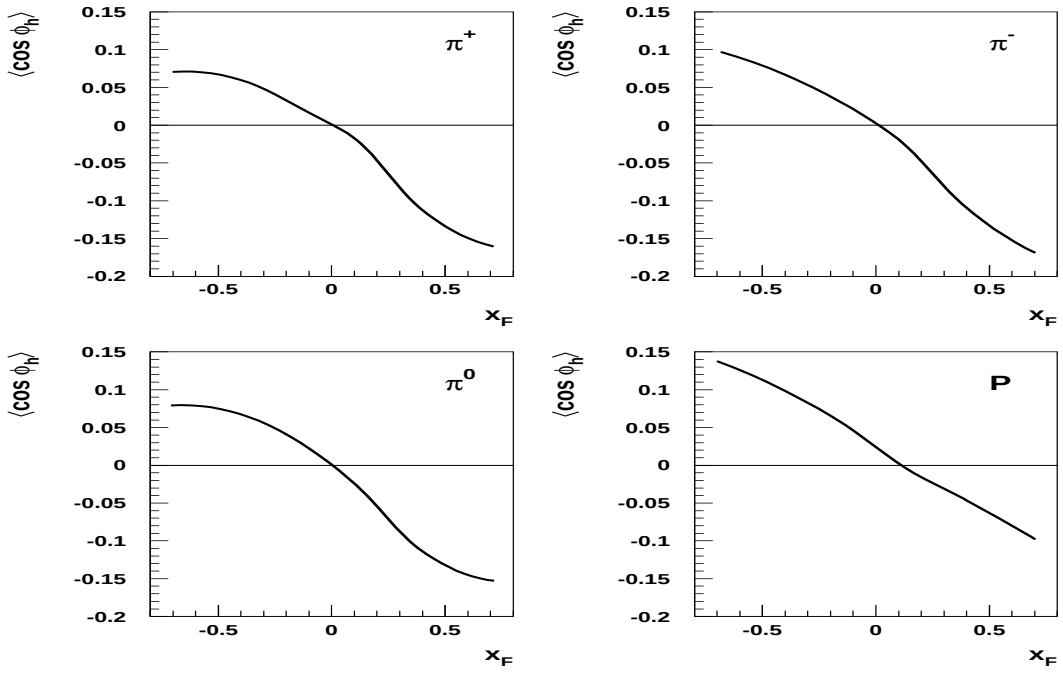

Figure 6: The $\cos\phi$ azimuthal moment for different hadrons in CLAS12 kinematics ($E_{Beam} = 11GeV$) as a function of x_F [57]. Negative x_F represent the target fragmentation.

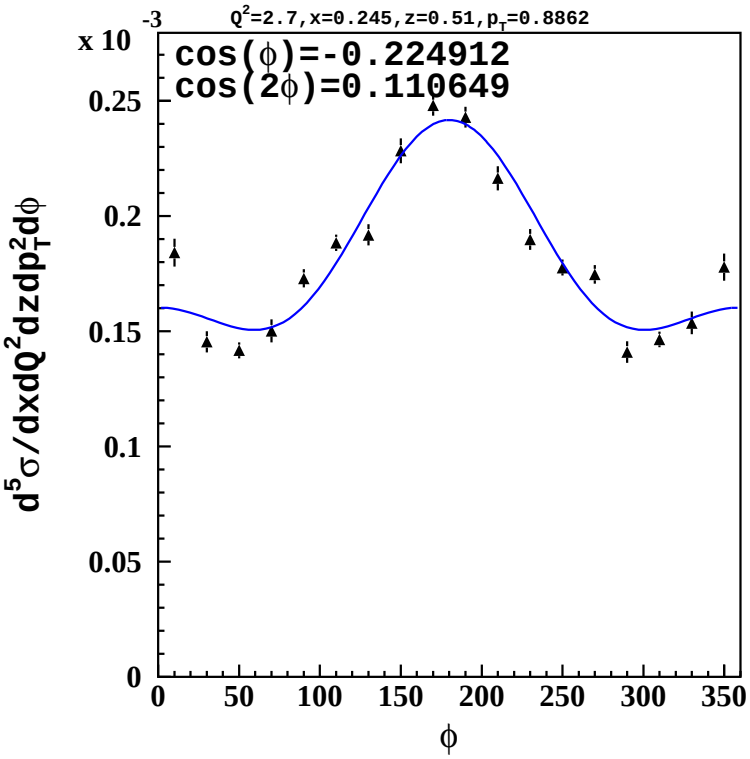

Figure 7: The preliminary data on azimuthal moments from CLAS E16 experiment at 5.7 GeV..

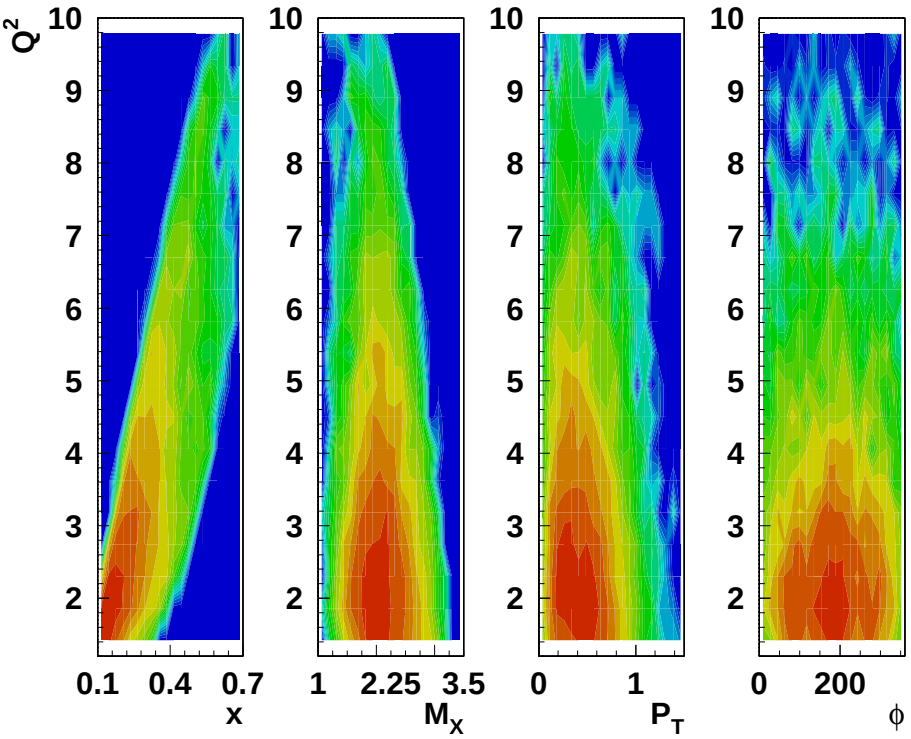

Figure 8: The kinematic coverage of CLAS12 for $e\pi^+X$.

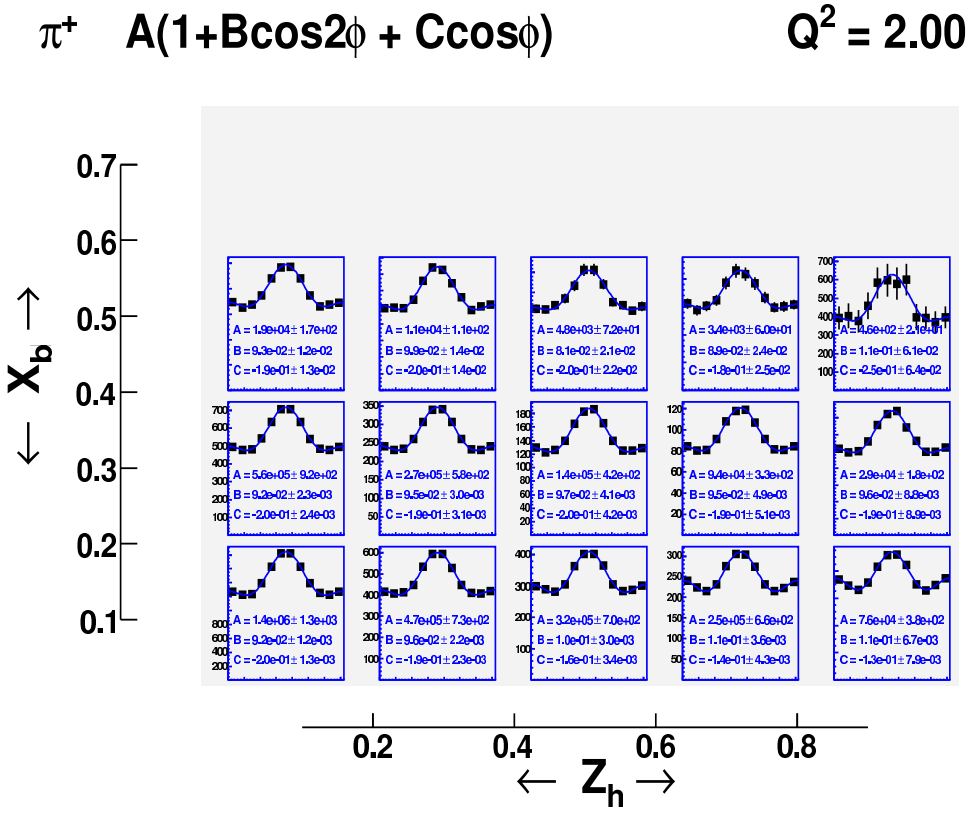

Figure 9: Simulated cross sections for the reaction $ep \rightarrow e\pi^+X$. The data were fit with the function $A(1 + Bcos2\phi + Ccos\phi)$ to obtain the parameters A, B and C

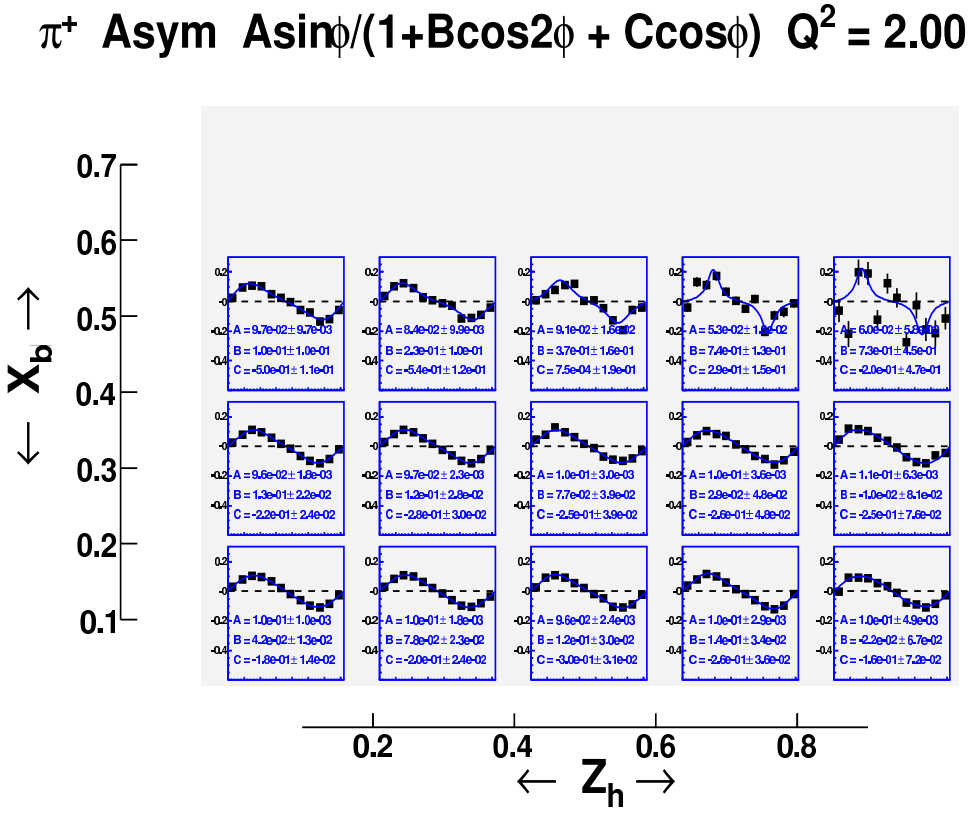

Figure 10: Simulated asymmetries and fits to $A\sin\phi/(1+Bcos2\phi+Ccos\phi)$ for the reaction $ep \to e\pi^+X$ at $Q^2 = 2\ GeV^2$.

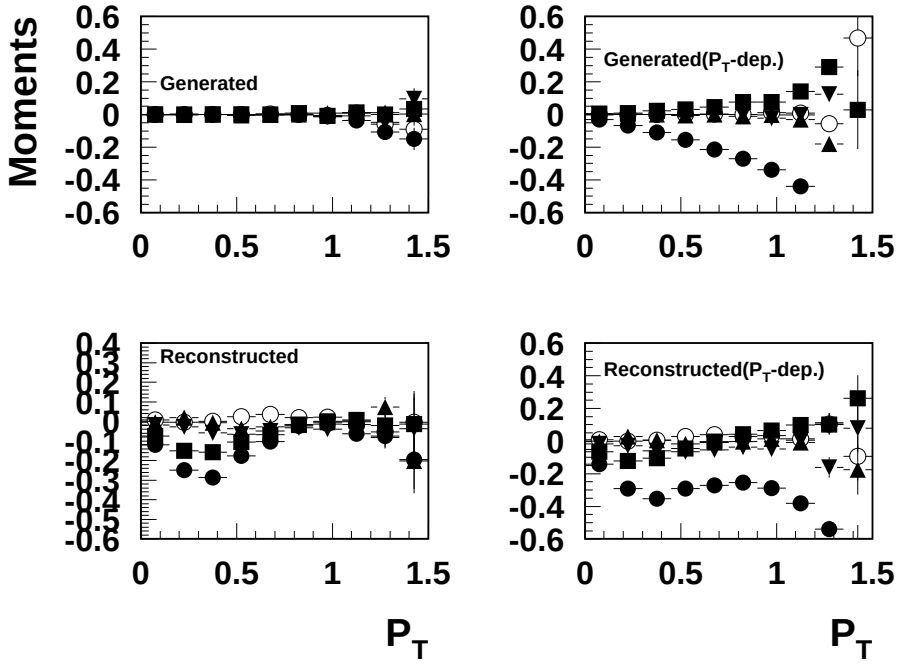

Figure 11: Extracted azimuthal moments for $e\pi^+X$ using the PEPSI-MC with (right panel) and without (left panel) account of azimuthal moments in the cross section. Circles,squares, triangles up and down are for $< cos\phi >, < cos2\phi >, < cos3\phi >, < cos4\phi >, < cos5\phi >$ respectively.

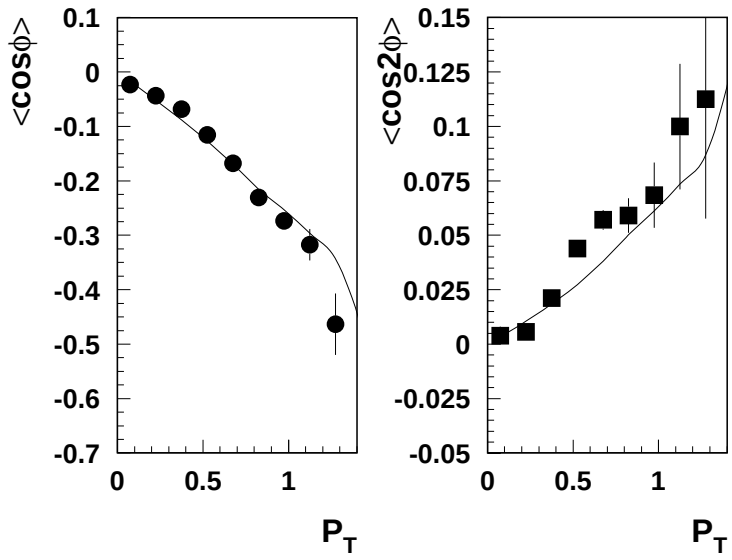

Figure 12: Extracted $< cos\phi >$ and $< cos2\phi >$ moments of the $e\pi^+X$ cross section from the MC-data (circles) compared to initial moments used as input in the PEPSI-MC (curves).

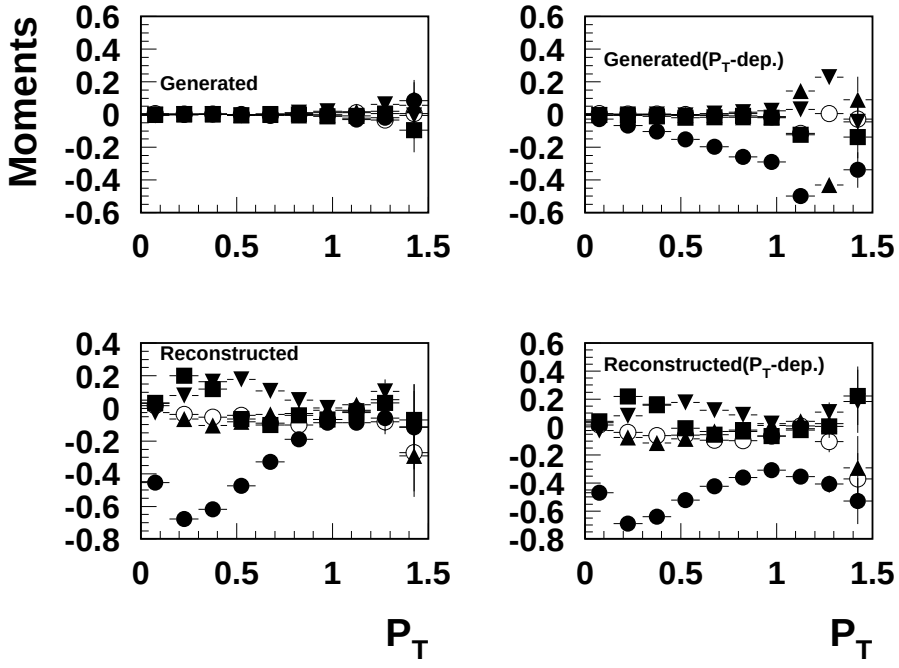

Figure 13: Extracted azimuthal moments for $e\pi^- X$ using the PEPSI-MC with (right panel) and without (left panel) account of azimuthal moments in the cross section. Circles,squares, triangles up and down are for $< cos\phi >, < cos2\phi >, < cos3\phi >, < cos4\phi >, < cos5\phi >$ respectively.

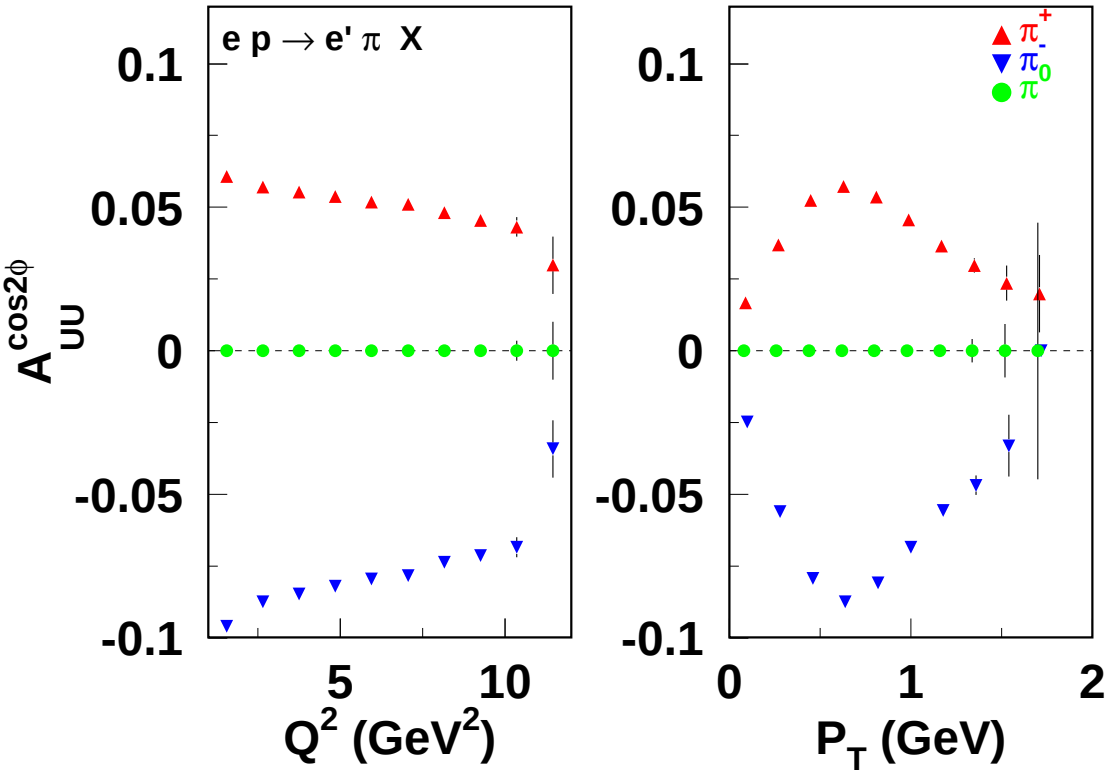

Figure 14: The $\cos 2\phi$ moment as a function of Q^2 for $0.5 < P_T < 0.6$ (left) and the P_T for $4. < Q^2 < 5.$ (right) at 11 GeV for pions from 2000h of CLAS12. Values are calculated assuming $H_1^{\perp u\to\pi^+} = -H_1^{\perp u\to\pi^-}$.

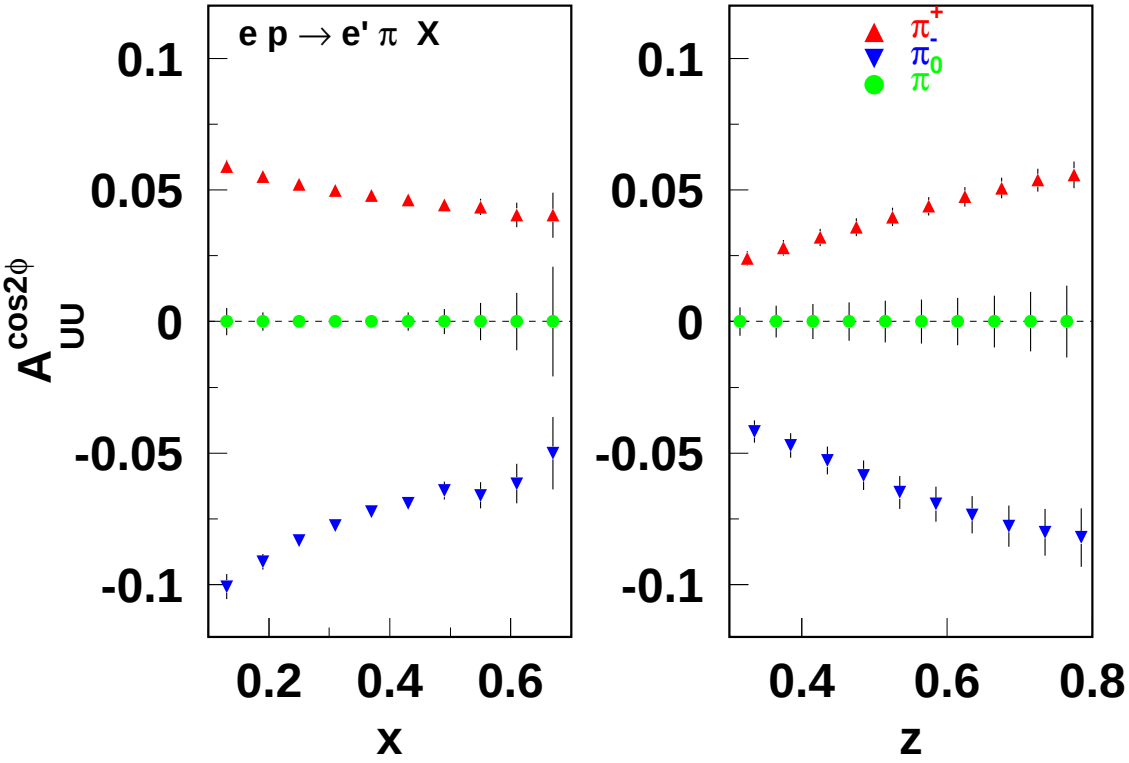

Figure 15: The $\cos 2\phi$ moment as a function of x for $0.8 < P_T < 0.9, 0.5 < z < 0.55$ (left) and the z for $0.35 < x < 0.4, 0.8 < P_T < 0.9$ (right) at 11 GeV for pions from 2000h of CLAS12.

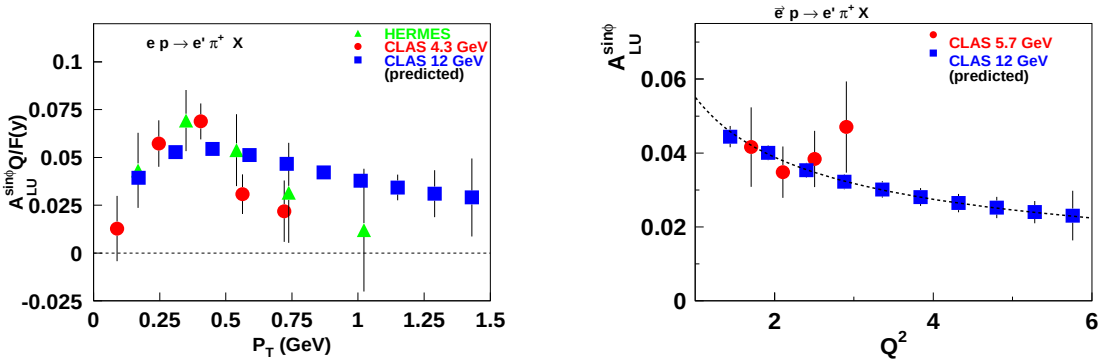

Figure 16: Beam SSA measured as a function of the transverse momentum of the π^+ (left) and momentum transfered Q^2 (right). The P_T-dependent SSA is corrected for the kinematic factor $F(y)$ accounting different average y in two experiments.

References

[1] K. Heller *et al.* 'Proceedings of Spin 96',Amsterdam,Sep.1996,p23

[2] Fermilab E704 collaboration (A. Bravar *et al.*), Phys.Rev.Lett. **77**, 2626 (1996).

[3] HERMES collaboration (A. Airapetyan *et al.*), Phys.Rev.Lett. **84**, 4047 (2000).

[4] HERMES collaboration (A. Airapetyan *et al.*), Phys.Rev. **D64**, 097101 (2001).

[5] HERMES collaboration (A. Airapetyan *et al.*), Phys.Rev.Lett. **94**, 012002 (2005).

[6] COMPASS collaboration (V.Yu. Alexakhin *et al.*), Phys.Rev.Lett. **94**, 202002 (2005).

[7] CLAS Collaboration (H. Avakian *et al.*) Phys. Rev. **D69**, 112004 (2004).

[8] S. Brodsky *et al.*, Phys. Lett. B **530**, 99 (2002).

[9] J. Collins, Phys. Lett. B **536**, 43 (2002).

[10] X. Ji, F. Yuan, Phys. Lett. B **543**, 66 (2002).

[11] A. Belitsky,X. Ji and F. Yuan, Nucl. Phys. **B 656**, 165 (2003).

[12] D. Boer, P. J. Mulders and F. Pijlman, Nucl. Phys. B **667**, 201 (2003).

[13] X. Ji, J-P. Ma and F. Yuan, e-Print Archive: hep-ph/0404183;

[14] J. C. Collins and A. Metz, e-Print arXiv:hep-ph/0408249. Phys. Lett. B **597**, 299 (2004), e-Print arXiv: hep-ph/0405085.

[15] X. Ji, J. P. Ma and F. Yuan, Nucl. Phys. B **652**, 383 (2003).

[16] D. Sivers, Phys.Rev. **D43**, 261 (1991).

[17] M. Anselmino and F. Murgia, Phys. Lett. B **442**, 470 (1998).

[18] S. Brodsky *et al.*, Nucl. Phys. **B 642**, 344 (2002).

[19] M. Burkardt, Phys.Rev. **D72**, 094020 (2005).

[20] M.Gockeler et al., Nucl.Phys.Proc.Suppl.153,146 (2006); hep-lat/0512011.

[21] R.N. Cahn, Phys. Lett. **B78** (1978) 269; Phys. Rev. **D40** (1989) 3107.

[22] M. Anselmino, M. Boglione, U. D'Alesio, A. Kotzinian, F. Murgia and A. Prokudin, Phys. Rev. D **71**, 074006 (2005) [arXiv:hep-ph/0501196]; Phys. Rev. D **72**, 094007 (2005) [Erratum-ibid. D **72**, 099903 (2005)] [arXiv:hep-ph/0507181].

[23] A. Kotzinian, B. Parsamyan and A. Prokudin, arXiv:hep-ph/0603194.

[24] M. Anselmino, A. Efremov, A. Kotzinian and B. Parsamyan (article in preparation).

[25] A. Bacchetta, M. Boglione, A. Henneman and P. J. Mulders, Phys. Rev. Lett. **85**, 712 (2000) [arXiv:hep-ph/9912490].

[26] L.Elouadrhiri et al., The CLAS12 Spectrometer: Components and Performance.

[27] H. Georgi, H.D. Politzer, Phys. Rev. Lett. **40** (1978) 3.

[28] A. Mendez, Nucl. Phys. **B145** (1978) 199.

[29] A. König, P. Kroll, Z. Phys. **C16** (1982) 89.

[30] J. Chay, S.D. Ellis, W.J. Stirling, Phys. Rev. **D45** (1992) 46.

[31] E.L. Berger, Z. Phys. **C 4**, 289 (1980)

[32] A. Brandenburg, V. Khoze, D. Muller Phys. Lett. B **347**, 413 (1995)

[33] A. Afanasev, C. E. Carlson and C. Wahlquist, Phys. Lett. B **398**, 393 (1997); Phys. Rev. D **58**, 054007 (1998).

[34] S. J. Brodsky, M. Diehl, P. Hoyer and S. Peigne, Phys. Lett. B **449**, 306 (1999)

[35] D. Boer and P. Mulders, Phys.Rev. **D57**, 5780 (1998).

[36] J. Collins, Nucl. Phys. **B396**, 161 (1993).

[37] R.D. Tangerman and P.J. Mulders, Phys.Rev. D**51** 3357 (1995).

[38] K.A. Oganessyan, H.R. Avakian, N. Bianchi, P. Di Nezza, Eur. Phys. J. **C5** (1998) 681.

[39] L.P. Gamberg, G.R. Goldstein, K.A. Oganessyan, Phys. Rev. **D67** (2003) 071504. L. Gamberg, hep-ph/0412367.

[40] V. Barone, Z. Lu and B. Q. Ma, Phys. Lett. B **632**, 277 (2006) [arXiv:hep-ph/0512145].

[41] NA10 Collaboration, S. Falciano, et al., Z. Phys. **C31** (1986) 513;
NA10 Collaboration, M. Guanziroli, et al., Z. Phys. **C37** (1988) 545.

[42] E615 Collaboration, J.S. Conway, et al., Phys. Rev. **D39** (1989) 92.

[43] Z. Lu, B.-Q. Ma, Phys. Rev. **D70** (2004) 094044;

[44] Z. Lu, B.-Q. Ma, Phys. Lett. **B615** (2005) 200 (hep-ph/0504184).

[45] R. Jakob, P.J. Mulders, J. Rodrigues, Nucl. Phys. **A626** (1997) 937.

[46] A. Bacchetta, A. Schäfer, J.-J. Yang, Phys. Lett. **B578** (2004) 109.

[47] ZEUS Collaboration, J. Breitweg, et al., Phys. Lett. **B481** (2000) 199.

[48] X. Ji, J. Qiu, W. Vogelsang and F. Yuan, Phys.Rev. D73, 094017 (2006); Phys. Lett. B **638**, 178 (2006).

[49] D. Boer, Nucl. Phys. **B603** (2001) 195.

[50] A. Afanasev, C. E. Carlson and C. Wahlquist, Phys. Rev. D **62**, 074011 (2000).

[51] F. Yuan, Phys. Lett. B **589**, 28 (2004).

[52] L. Gamberg et al. (2004).

[53] A. Afanasev and C. Carlson, hep-ph/0308163.

[54] A. Bacchetta, P. Mulders and F. Pijlman Phys. Lett. **B 595**, 309 (2004).

[55] HERMES collaboration, in preparation.

[56] A. Efremov *et al.*, Phys. Rev. D67, 114014 (2003).

[57] A. Kotzinian, hep-ph/0510359.

[58] EMC, M. Arneodo, et al., Z. Phys. **C34** (1987) 277.

[59] Adams et al, E665 Collaboration, Phys. Rev. **D48**, 5057 (1993).

[60] HERMES collaboration, in preparation.

[61] I. Akushevich, N. Shumeiko and A.Soroko EPJ, hep-ph/9903325

[62] A.M. Kotzinian and P.J. Mulders, Phys. Rev. D**54** 1229 (1996).

[63] H.Avakian et al. "Semi-Inclusive Pion Production with a Longitudinally Polarized Target at 12 GeV", Letter of Intent to Jefferson Lab PAC 30.

[64] H.Avakian et al. "Semi-Inclusive Pion Production with a Transversely Polarized Target at 12 GeV", Letter of Intent to Jefferson Lab PAC 30.

[65] BELLE Colaboration, K.Abe et al, hep-ex/0705063.

[66] P.B. van der Nat and K. Griffioen. hep-ex/0501009.

[67] R. L. Jaffe, X. Jin, and J. Tang, Phys. Rev. Lett. **80**,1166 (1998).

[68] A. Bacchetta and M. Radici Phys. Rev. **D 67**, 094002 (2003).

Appendix: Moments and the acceptance

The double polarized cross section and the acceptance can be expanded in Fourier series.

$$\sigma(\phi)/\sigma_0 = a_0 + \sum_m a_m \times cos(m\phi) + \sum_n b_n \times sin(n\phi) \tag{10}$$

$$A(\phi)/A_0 = 1 + \sum_l A_l \times cos(l\phi) + \sum_k B_k \times sin(k\phi) \tag{11}$$

The σ_0 is the ϕ integrated cross section and A_0 is the ϕ integrated acceptance factor.

Using the normalized measured cross section $\sigma_M(\phi)= \sigma(\phi)A(\phi)/\sigma_0 A_0$ one can obtain

$$\begin{aligned}
\sigma_M(\phi) = a_0 + \frac{1}{2}\sum_i (A_i a_i + B_i b_i) + \qquad (12)\\
cos\phi \left[a_1 + a_0 A_1 + \frac{1}{2}\sum_i (A_i a_{i+1} + a_i A_{i+1} + B_i b_{i+1} + b_i B_{i+1})\right] +\\
sin\phi \left[b_1 + a_0 B_1 + \frac{1}{2}\sum_i (B_i a_{i+1} - a_i B_{i+1} + A_i b_{i+1} - b_i A_{i+1})\right] +\\
cos(2\phi) \left[a_2 + a_0 A_2 + \frac{1}{2}\sum_i (A_i a_{i+2} + a_i A_{i+2} + B_i b_{i+2} + b_i B_{i+2}) + a_1 A_1 - b_1 B_1\right] +\\
sin(2\phi) \left[b_2 + a_0 B_2 + \frac{1}{2}\sum_i (-B_i a_{i+2} + a_i B_{i+2} + A_i b_{i+2} - b_i A_{i+1}) + a_1 B_1 + b_1 A_1\right] +\\
cos(3\phi)\,[a_3 + a_0 A_3 + ...] +\\
sin(3\phi)\,[b_3 + a_0 B_3 + ...] +\\
.....
\end{aligned}$$

Three methods are used to extract the b_1 term (acceptance corrections could be seen in comparison of 2 different beam spin states ($\lambda_e = \pm 1$)).

In method I

$$\frac{\int \sigma_M(\phi) sin\phi d(\phi)}{\int \sigma_M(\phi) sin^2(\phi) d(\phi)} = \frac{\sum sin(\phi_i) W_i}{\sum sin^2(\phi_i) W_i} = b_1 + a_0 B_1 ..., \tag{13}$$

where W_i is the weight of the i-th event (including dead time corrected luminosity).

In method II

$$\frac{\int \sigma_M(\phi) sin\phi d(\phi)}{\int \sigma_M(\phi) d(\phi)} = \frac{\sum sin(\phi_i) W_i}{\sum W_i} = (b_1 + a_0 B_1)/2 + ..., \tag{14}$$

In method III

$$\frac{\int_0^\pi \sigma_M(\phi) d(\phi) - \int_\pi^{2\pi} \sigma_M(\phi) d(\phi)}{\int_0^\pi \sigma_M(\phi) d(\phi) + \int_\pi^{2\pi} \sigma_M(\phi) d(\phi)} = \frac{N(\phi < \pi) - N(\phi > \pi)}{N(\phi > \pi) + N(\phi < \pi)} = 2(b_1 + a_0 B_1)/\pi + ... \tag{15}$$

The biggest term contained in the $\cdots$ is $A_1 b_2$. The value of A_1 is ≈ 0.3. The value of the b_2 was estimated theoretically and measured experimentally to be less than 5%, so the final contribution of the product to $\langle sin\phi \rangle$ is negligible.